Nature of the Inactivation of Elastase by *N*-Peptidyl-*O*-aroyl hydroxylamine as a Function of pH[†,‡]

Xiaochun Ding,[§] Bjarne F. Rasmussen,[∥,○] Hans-Ulrich Demuth,[#] Dagmar Ringe,[*,⊥,§,○] and Anke C. U. Steinmetz[▽]

Departments of Chemistry and Biochemistry, Rosenstiel Basic Medical Sciences Research Center, and Program in Biophysics, Brandeis University, Waltham, Massachusetts 02254

Received December 6, 1994; Revised Manuscript Received March 17, 1995[⊗]

ABSTRACT: The mechanism of inactivation of porcine pancreatic elastase (PPE) by *N*-peptidyl-*O*-aroylhydroxylamine was studied by X-ray crystallography. The inactivator forms a stable complex with the enzyme by means of a covalent attachment to the active site Ser 203(195) Oγ. The nature of the complex is, however, different depending on the pH at which the inactivation reaction occurs. At pH 5, the complex formed is a hydroxylamine derivative of Ser 203(195) in which the Oγ of serine is the oxygen of the hydroxylamine derivative. At pH 7.5, the complex formed is a carbamate derivative at Ser 203(195)Oγ. In both types of complexes, the inactivator binds in the S′ subsites of the enzyme instead of forming the usual antiparallel β-sheet with the S subsites. The implication for the mechanism of inactivation at different pHs is discussed.

N-Peptidyl-*O*-aroylhydroxylamines are mechanism-based inactivators of serine and cysteine proteases (Demuth et al., 1989). They can react with these enzymes by two parallel pathways (Scheme 1): enzyme-catalyzed hydrolysis of the pseudosubstrate or inactivation of the enzyme. Thus, in pathway I, the target enzyme hydrolyzes the compound as a substrate. The final products are active enzyme, peptide and the *O*-acylhydroxylamine. In pathway II, the compound inactivates the enzyme. However, a number of different mechanisms are possible. In one case, the hydroxylamine compounds undergo enzyme-induced decomposition at the NH−O linkage to produce a reactive nitrene intermediate. This intermediate can then react further with an active site residue of the enzyme. For instance, if a serine reacts directly with the nitrene intermediate, a hydroxylamine derivative involving the inactivator and enzyme will result (pathway II_1). If the nitrene intermediate proceeds through a Lossen-type rearrangement to give an isocyanate intermediate, and a serine on the enzyme reacts with this new intermediate a carbamate derivative will result (pathway II_2) (Fischer et al., 1983; Demuth et al., 1991). An alternative pathway has been suggested for the reaction of diacylhydroxylamine inhibitors with papain and may be applicable to serine proteases. In this pathway, the γ-sulfur of cysteine attacks the carbonyl group of the P1 residue to give a tetrahedral intermediate. Inactivation results from the migration of the γ-sulfur of cysteine to the hydroxylamine nitrogen, giving a sulfenamide derivative (Robinson et al., 1991; Smith et al., 1988). The partition ratio between the two processes (pathway I/pathway II) is a characteristic measure of mechanism-based inactivators. For instance, in the reaction of dipeptidylpeptidase IV with these types of compounds, this ratio is in the range of 10^4-10^6. For PPE[1] and subtilisin, only inactivation is observed (Demuth et al., 1988).

So far, the products of the inactivation by these types of compounds have been established unequivocally not only for a cysteine protease but also for a serine protease (subtilisin) (Steinmetz et al., 1994). The structure of subtilisin inactivated with a *N*-peptidyl-*O*-aroylhydroxylamine inhibitor has been solved at pH 7.5 (Steinmetz et al., 1994). The covalent complex which forms under these conditions is the carbamate derivative between inactivator and enzyme. Subtilisin belongs to the subtilisin family of serine proteases, elastase belongs to the trypsin family of serine proteases. These two families have their catalytic functional groups arranged in the same geometrical relationship, even though they have entirely different overall three-dimensional structures. All previous evidence indicates that they catalyze the hydrolysis of peptides by the same reaction sequence, which includes a Michaelis complex, tetrahedral, and acyl-enzyme intermediates (Kraut 1977; Ding et al., 1994). The cysteine proteases have a similar arrangement of catalytic groups, except that serine is replaced by cysteine. The same mechanism of hydrolysis is postulated (Robinson et al., 1991). So it is not surprising that both types of proteases are inactivated by this type of compound.

However, the product of inactivation is quite different for these two types of proteases (Robinson et al., 1991; Steinmetz et al., 1994). In studying the inactivation of elastase by these compounds, we have found that the products of inactivation can also be different among the serine proteases. The differences in mechanism that lead to these products in the

[†] Supported in part by a grant from the Lucille P. Markey Charitable Trust and by a grant from the National Institutes of Health (GM-26788)

[‡] The atomic coordinates are available from the Brookhaven Protein Data Bank under entry codes 1ELF and 1ELG.

* Author to whom correspondence should be addressed.

[§] Department of Chemistry.

[∥] Present address: c/o I.L.L. B.P. 156X, 38042 Grenoble Cedex 9, France.

[⊥] Department of Biochemistry.

[#] Present address: Hans Knoell Institut für Naturstoffforschung, Arbeitsgemeinschaft Wirkstoffbiochemie Halle, Halle, Germany.

[▽] Program in Biophysics.

[○] Rosenstiel Basic Medical Sciences Research Center.

[⊗] Abstract published in *Advance ACS Abstracts,* May 15, 1995.

[1] Abbreviations: Boc-ALA2-ALA1-NHO-Nb, *N*-(*tert*-butoxycarbonylalanylalanyl)-*O*-(*p*-nitrobenzoyl)hydroxylamine; PPE, porcine pancreatic elastase. Ser 203 is the active site serine of elastase. The equivalent residues in chymotrypsinogen are given in parentheses. Thus, Ser 203(195) corresponds to Ser 195 in chymotrypsinogen.

0006-2960/95/0434-7749$09.00/0

Scheme 1

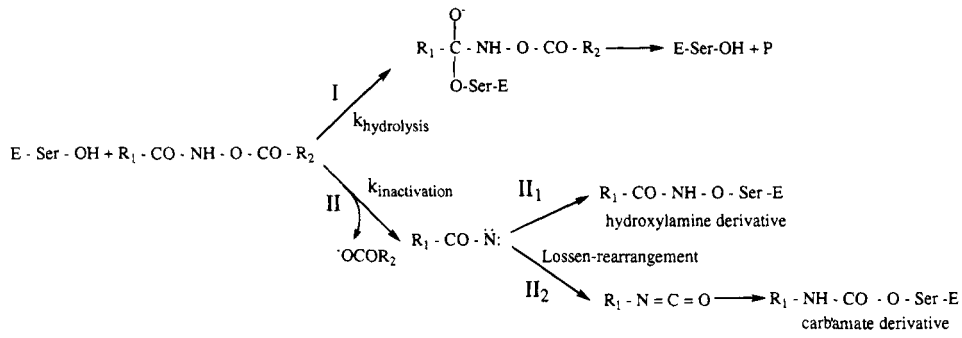

serine and cysteine proteases should reflect the differences in the nucleophilicity of the active site serine or cysteine. However, differences in reactivity of the serine proteases can only be due to differences in either binding mode of inhibitor to enzyme or by differences in conditions at which the reactions occur. To address this issue, the structures of porcine pancreatic elastase (PPE) inactivated by Boc-ALA2-ALA1-NHO-Nb at two different pHs have been studied.

The productive, forward binding mode of a peptide substrate/inhibitor to elastase is characterized by antiparallel β-pleated sheet formation between the peptide and strand 222(214)−224(216) of the enzyme as seen for other serine protease/inhibitor complexes (Ding et al., 1994; Takahashi et al., 1988). These interactions would position the carboxyl terminus of a substrate or inhibitor in a favorable position for nucleophic attack at the carbonyl carbon by the γ-oxygen of Ser 203(195). Multiple binding modes and backward binding with noncovalent short peptide complexes have been observed for PPE. For example, Ac-Pro-Ala-Pro-Tyr-NH2 (Clore et al., 1986) binds in the S′ subsites of the active site, two molecules of Ac-Ala-Pro-Ala (Meyer et al., 1986) bind backward in both S and S′ subsites of the active site, and a series of inhibitors, the trifluoroacetyldipeptide anilides, have been found to bind backward in the S subsites of the enzyme (Mattos, 1994). However, the assumption of productive binding modes is thought to be true for covalent inhibitors. In order to react with the active site nucleophile of the enzyme, the inhibitor should be oriented in the same way as the substrate for the reactive group to be close enough to an active site residue of the enzyme. This simple view is complicated by experiments with heterocyclic inactivators. For example, the structure of the complex formed between PPE and 4-chloro-3-ethoxy-7-guanidinoisocoumarin (Powers et al., 1990) shows that the ethoxy group binds in the S1 subsite, but the guanidinoisocoumarin group of the inhibitor binds in an S′ subsite. These results indicate either that PPE can accommodate different binding modes and still react with inhibitors to form covalent complexes or that inhibitors rearrange conformationally after reaction. The specific binding mode of an inhibitor may therefore depend on the detailed structure of the compound. Another example of an unusual binding mode occurs in the structure of subtilisin inactivated with *N*-(*tert*-butoxycarbonylalanylprolylphenyl)-*O*-benzoyl hydroxylamine (Steinmetz et al., 1994). The peptide part of the inactivator is not able to form the usual antiparallel β-sheet in the S subsites as postulated for the enzyme−substrate complex. Instead, the proline, alanine, and *tert*-butoxycarbonyl groups of the inactivator protrude out of the active site into solvent. The influence of binding mode in directing the mode of inactivation by these hydroxylamine inactivators is therefore a very important consideration in evaluating the mechanism by which inactivation occurs.

MATERIALS AND METHODS

PPE was obtained from Worthington Biochemicals and was used without further purification. The inactivator Boc-ALA2-ALA1-NHO-Nb (A) was provided by H.-U.D.

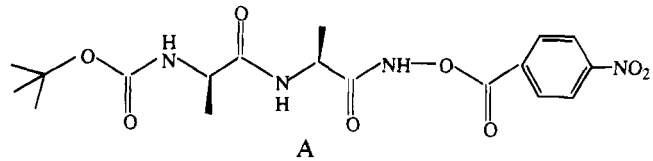

A

Crystallization

Crystals of PPE Inactivated with Boc-ALA2-ALA1-NHO-Nb at pH 5. PPE was co-crystallized with the inactivator at pH 5 by the method of vapor diffusion using the sitting drop method. Crystals were grown in 18−24 μL drops with 0.52 mM inactivator (K_i = 0.12 mM), 1.4 mM sodium sulfate, and 100 mM sodium acetate. The PPE concentration varied from 6.8 to 8.3 mg/mL. The reservoir consisted of 15 mL of a 100 mM sodium sulfate and 100 mM acetate buffer at pH 5.

Crystals of PPE Inactivated with Boc-ALA2-ALA1-NHO-Nb at pH 7.5. Native PPE was crystallized by the method of vapor diffusion using the sitting drop method. Crystals were grown in 18−24 μL drops containing 5−11 mM sodium sulfate and 10 mM sodium acetate at pH 5. The PPE concentration varied from 6.0 to 7.4 mg/mL. The reservoir consisted of 15 mL of a 20 mM sodium sulfate, 10mM acetate buffer at pH 5. The native PPE crystals were then transferred to 10 mM sodium sulfate, 0.6 M phosphate buffer at pH 7.5. Crystals of PPE were inactivated with Boc-ALA2-ALA1-NHO-Nb by adding the inactivator to the mother liquor at a final concentration of 0.7 mM and allowing them to soak for 2 days at 4 °C. To avoid spontaneous degradation of inactivator, solution containing fresh inactivator was added several times daily.

Data Collection

Table 1 shows the data collection and refinement statistics for the structures reported here. For the structure of the PPE−inactivator complex at pH 5, data were collected to 1.65 Å resolution at −6 °C using ω scans on a Siemens P3 diffractometer outfitted with an LT-1 low temperature device. Two crystals were used for data collection. The first crystal had approximate dimensions of 0.5 mm × 0.3 mm × 0.3

Table 1: Data Collection and Refinement Statistics for the Structures of the PPE/Boc-ALA2-ALA1-NHO-Nb Complexes at pH 5 and 7.5

	derivative formed at pH 5	derivative formed at pH 7.5
	Data Collection	
space group	$P2_12_12_1$	$P2_12_12_1$
unit cell	$a = 51.08$, $b = 58.04$, $c = 75.18$, $\alpha = \beta = \gamma = 90°$	$a = 51.27$, $b = 58.09$, $c = 75.33$, $\alpha = \beta = \gamma = 90°$
molecules per asymmetric unit	1	1
resolution (Å)	44−1.65	22.36−1.68
total no. reflections ($I/\sigma(I) > 0$)	27890	23713
completeness	100%	91%
	Refinement Statics	
resolution range (Å)	10−1.65	10−1.68
no. of reflections ($I/\sigma(I)$)	23730 (2σ)	21705 (1σ)
completeness	85%	84%
R-factor ($=\Sigma\|\|F_o\| - \|F_c\|\|/\Sigma\|F_o\|$)	0.17	0.18
rms deviations		
bond length (Å)	0.013	0.014
bond angles (deg)	2.6	3.9
average B factor		
main chain	9.6	10.9
side chain	14.2	15.0
water	26.6	26.8
inhibitor	44.6	16.9 (0.5 occupancy)
total no. of		
protein atoms	1822	1822
waters	189	160
inhibitor atoms	18	18

mm and was used to collect data to 2.0 Å resolution. The second crystal had approximate dimensions of 1.0 mm × 0.5 mm × 0.3 mm and was used to collect high resolution data. A total of 27 890 unique reflections corresponding to 100% of the expected reflections to 1.65 Å were obtained. Background intensity was measured using a block of representative reflections which cover the resolution range. Also, a different block of reflections which cover the resolution range was collected at the beginning and end of data collection in order to correct for radiation decay. During the data processing, correction for absorption, radiation decay, background, and Lorentzian polarization were applied.

For the structure of the PPE−inactivitor complex at pH 7.5, diffraction data to 1.68 Å resolution were collected at 4 °C on a Xentronics area detector from one crystal with dimensions of 0.5 mm × 0.3 mm × 0.3 mm. The data were reduced with program XDS (Kabsch, 1988). The overall R_{merge} for the data set is 10.0%.

Refinement

The PPE−Inactivator Complex at pH 5. Initial phases were calculated from coordinates taken from PDB entry no. pdb3est.ent (Bernstein et al., 1977) from a structure determination by Meyer et al. (1988) from which all solvent molecules had been removed. These phases, together with data [$I/\sigma(I) > 1$] from the first crystal to 2.0 Å resolution, gave an initial model with overall starting R factor of 28.7% and an overall isotropic temperature factor of 6.2 Å, using PROLSQ (Hendrickson & Konnert, 1978; Konnert & Hendrickson, 1980). A difference Fourier electron density map with coefficients $2|F_o| - |F_c|$ was calculated. The model of the protein fitted the electron density nicely. There was clear electron density in the active site contiguous with the electron density of the Oγ of Ser 203(195), indicating a covalent derivative of the enzyme. There was no density which could be interpreted as a leaving group. Refinement against the data to 2.0 Å was continued with individual isotropic temperature factors using PROLSQ, combined with manual rebuilding, causing the R factor to drop to 17.8%. A difference Fourier electron density map with coefficients $|F_o| - |F_c|$ was calculated. In this map the water molecules and ions that were previously excluded from the initial model were added. Only the water molecules present at a contour level of 3σ were retained. In addition, the structural calcium ion was identified. The refinement was continued with all data [$I/\sigma(I) > 1$] between 10 and 1.65 Å resolution from both crystals. The overall isotropic temperature factor increased to 8.6 Å with an R factor of 28.3%. Subsequent rounds of refinement with individual isotropic temperature factors and addition of more water molecules using program WATERHUNTER (Sugio, unpublished) gave a model with an R factor of 20.7%. At this stage, a difference Fourier electron density map with coefficients $2|F_o| - |F_c|$ was clear enough to build in a model of the inactivator. An energy-minimized initial model for the inactivator was built using QUANTA (Molecular Simulations Inc.). An Evans & Sutherland PS300 graphics system and program FRODO (Jones, 1985) were used for positioning the inactivator into the electron density map. The electron density clearly shows an sp^2 conformation at the carbonyl group. But the covalent connection between this group and the Oγ of Ser 203(195) could only be modeled with reasonable geometry by inserting an additional atom, identified as a nitrogen based on the chemistry of the inhibitor. Therefore, the covalent linkage of the inactivator to the Oγ of Ser 203(195) was unambiguously identified as the hydroxylamine type. Refinement was continued with X-PLOR (Brünger et al., 1987; Brünger, 1988) using all data [$I/\sigma(I) > 2$] from 10 to 1.65 Å resolution. The parameters for energy minimization for this special type of hydroxylamine linkage were obtained as suggested by QUANTA. The final R factor is 17.3% with good geometry. The occupancy of inactivator is estimated at about 60% based on the electron density. An extra electron density next to the side chain of alanine is in the position of the water molecule of the native structure and was modeled as such. To confirm the results of the refinement, an omit map was calculated where the inhibitor and side chain atoms of active site residues Ser 203(195) and His 60(57) were deleted from the model. The electron density map produced confirmed the position of the inactivator. In order to ensure the linkage type, we refined the structure using the program TNT (Tronrud et al., 1987) with restraints based on geometry rather than energy. This refinement confirmed the hydroxylamine linkage. The nature of the chemical linkage supported by all of these types of refinement was the same.

The PPE−Inactivator Complex at pH 7.5. Initial phases were calculated from coordinates taken from PDB entry no. pdb3est.ent from a structure determination by Meyer et al. (1988) from which all solvent molecules and the side chains of the active site residues, serine and histidine, had been removed. These phases together with the data [$I/\sigma(I) > 1$] gave an initial model with overall starting R factor of 20.3% using X-PLOR. A difference Fourier electron density map with coefficients $|F_o| - |F_c|$ was calculated. Water mol-

ecules taken from the coordinates of the complex structure at pH 5 and ions that were previously excluded from the initial model were added. Only the water molecules present at a contour level of 3σ were retained. In addition, the structural calcium ion and sulfate ion on the exterior of the protein were identified. Refinement of this model gave an *R* factor of 18.6%. At this point a difference Fourier electron density map with coefficients $2|F_o| - |F_c|$ was calculated. The model of the protein fitted the electron density nicely. There was clear electron density in the active site contiguous with the electron density of the Oγ of Ser 203(195), indicating a covalent derivative of the enzyme. There was no density which could be interpreted as a leaving group. The residual electron density was interpreted in terms of a model for the inactivator partly overlapped by electron density for a sulfate ion. It is known that a sulfate ion binds in the active site of native PPE. Since the crystalline enzyme sample is only approximately 50% inactivated, half of the enzyme molecules still contain sulfate ion. In order to distinguish between the two proposed inactivated complexes, that is, between the carbamate and the hydroxylamine derivative, we first attempted to build the inactivator into the density as a hydroxylamine. In this model, the nitrogen atom of the hydroxylamine model went exactly into the density at which the sulfate ion overlaps. However, this model does not account for a density contiguous with and close to the Oγ of Ser 203(195) that can only be fitted with an sp^2 carbonyl group. On the other hand, the distance between the carbonyl carbon of ALA1 and the α-carbon of ALA1 is so far that an additional atom, identified as a nitrogen of the former hydroxylamine functional group, has to be inserted between the carbonyl carbon of ALA1 and the α-carbon of ALA1. Thus the nitrogen of the former hydroxylamine functional group and carbonyl group of ALA1 have rearranged, and the final covalent linkage must be a carbamate derivative. We refined the model further with inactivator and sulfate ion simultaneously in the active site region using X-PLOR, in which we restrain the inactivator and sulfate ion to be independent of each other, assigning each of them an occupancy of 0.5. In order to rule out the possibility that a hydroxylamine type complex coexists in the crystal, the following test was applied. A difference Fourier electron density map with coefficients $|F_o| - |F_c|$ calculated from a model containing only the carbamate type inactivator and sulfate ion should have no electron density for the rest of the inactivator if the model accounts for all of the density. Such a map did not show any extraneous density. Therefore, only the carbamate type complex formed at pH 7.5. Final refinement with X-PLOR and manual rebuilding give an *R* factor of 18.1% with good geometry.

RESULTS

The electron density clearly shows that the inactivator forms a covalent derivative with the γ-oxygen of Ser 203-(195) both at pH 5 and 7.5. At pH 5, only the hydroxylamine derivative (Figures 1a and 2b) has formed, in which the γ-oxygen of Ser 203(195) has replaced the oxygen of the hydroxylamine linkage and is now directly attached to the hydroxylamine nitrogen of the inactivator. At pH 7.5, a carbamate derivative (Figure 1b and 3b) has formed in which the hydroxylamine function of the inactivator and the carbonyl moiety of ALA1 have rearranged so that the hydroxylamine nitrogen is covalently bound between the former carbonyl carbon and α-carbon of ALA1, and the γ-oxygen of Ser 203(195) is attached to the former carbonyl carbon of ALA1.

There are no major changes in the structure of the protein as compared to the free enzyme. The root mean square differences for all backbone atoms (NCCO) between the structures of the complexes at pH 5 and 7.5 versus the free enzyme (PDB entry no. pdb3est.ent) are 0.2 and 0.2 Å, respectively.

Description of the Inactivated Derivative

The PPE−Inactivator Complex at pH 5. A model of the final refined structure of the complex at pH 5 is shown in Figure 2a. The inactivator binds in a groove on the surface of the protein that has been interpreted as the S′ side of the active site (Takahashi et al., 1988). In this derivative structure, the carbonyl oxygen of ALA1 does not bind in the "oxyanion hole" to form hydrogen bonds to the backbone amides of Gly 201(193) and Ser 203(195), as observed in other elastase−inhibitor structures. This might be due to the extra atom inserted between the carbonyl group of ALA1 and Oγ of Ser 203(195). However, the carbonyl oxygen of ALA1 forms a hydrogen bond with Nϵ2 of His 60(57) to further stabilize the hydroxylamine conformation. The position of the inactivator on the enzyme is stabilized by a covalent linkage between the enzyme and the inactivator and by noncovalent interactions between the peptide part of the inactivator and the protein (Figure 2b). These interactions include a hydrogen bond of 2.9 Å between the carbonyl oxygen of the hydroxylamine function and the nitrogen Nϵ2 of His 60(57) and a hydrogen bond of 2.9 Å between the amide nitrogen of ALA1 of the inactivator and the carbonyl oxygen of residue Thr 44(41). The positioning of the *tert*-butoxycarbonyl group of the inactivator is restrained by two different kinds of interactions. The first is the interaction of the *tert*-butoxycarbonyl group with a hydrophobic cavity close to the side chains of Leu 149(143) and Leu 156(151). The second is a system of hydrogen bonds involving two waters, the *tert*-butoxycarbonyl group, and the protein. One water molecule (WAT 972) hydrogen bonds to the carbonyl oxygen of the *tert*-butoxycarbonyl group (3.0 Å) and to the hydroxyl oxygen of Tyr 35(35) (2.6 Å). This water molecule is held in place by a hydrogen bond (3.0 Å) to another water molecule (WAT 729), which in turn hydrogen bonds (3.0 Å) to the carbonyl oxygen of His 43(40).

The PPE−Inactivator Complex at pH 7.5. A model of the final refined structure of the complex at pH 7.5 is shown in Figure 3a. The binding mode for the complex formed at pH 7.5 is similar to that of the complex formed at pH 5 with the peptide part located on the S′ side of the active site (Figure 4). However, at pH 7.5, the covalent linkage of the complex is of the carbamate type. The carbonyl oxygen of ALA1 is close to the oxyanion hole, forming a strong hydrogen bond with the amide nitrogen of Gly 201(193) (2.5 Å). The distance between this carbonyl oxygen and the amide nitrogen of Ser 203(195), the other residue contributing to oxyanion stabilization, is 3.3 Å, too far to be considered a hydrogen bond. Another hydrogen bond (3.0 Å) is formed between the carbonyl oxygen of residue Thr 44(41) and the amide nitrogen of ALA1 of the inactivator. Unlike the complex formed at pH 5, the *tert*-butoxycarbonyl

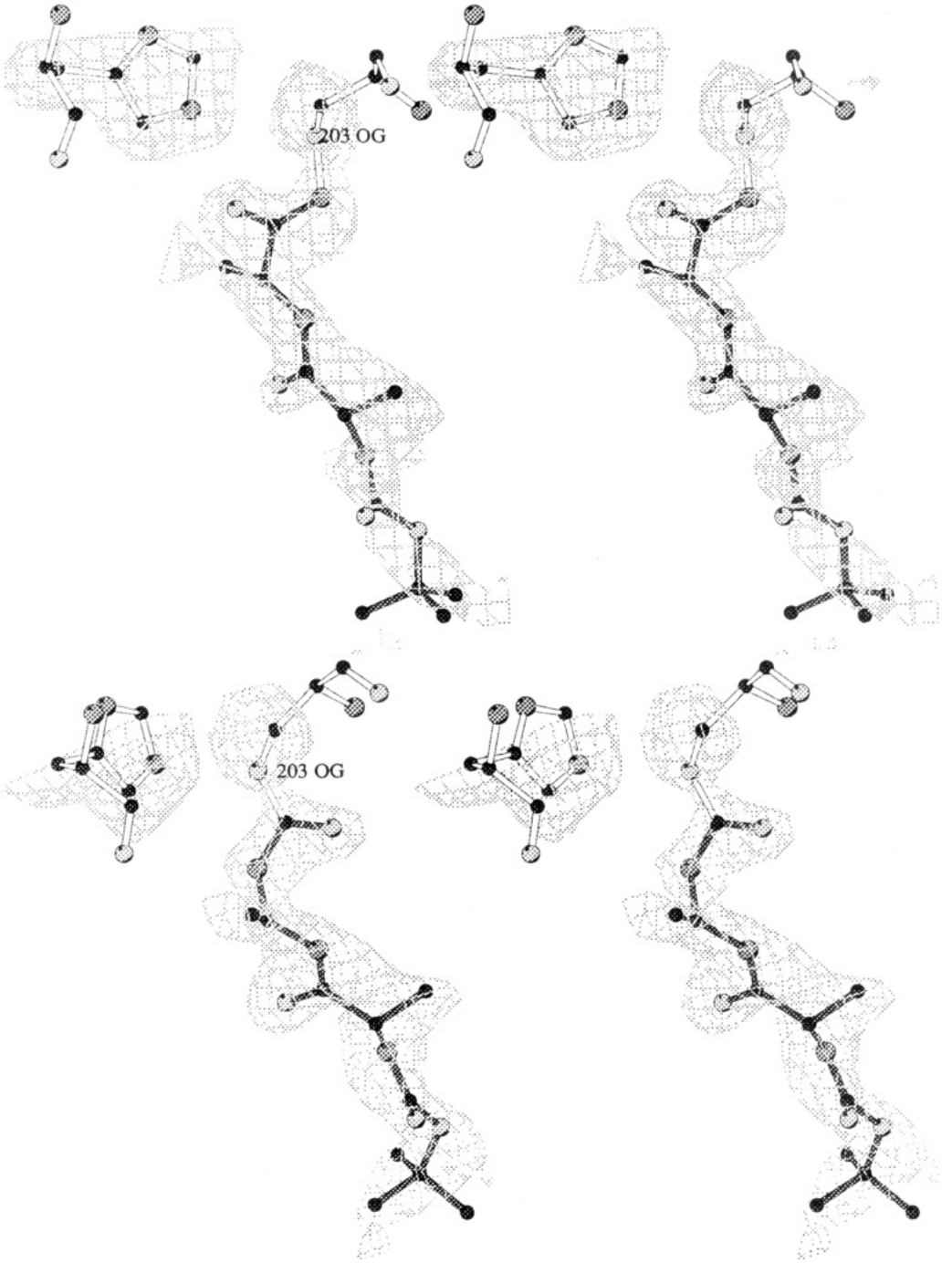

FIGURE 1: Final difference Fourier electron density maps with coefficients ($|F_o| - |F_c|$) of (a, top) the hydroxylamine/PPE complex formed at pH 5 and (b, bottom) the carbamate/PPE complex formed at pH 7.5. The maps were calculated with models from which the atoms of the side chains of Ser 203(195), His 60(57), and the atoms of the inactivators were omitted. Consequently, only the electron density corresponding to these atoms is shown for each. Superimposed on each electron density is the refined model of the complex, showing the positions of the atoms previously omitted. This view is rotated 90° from that of Figures 2 and 3 for clarity. The contouring level for the electron density maps is at 2.0σ. All figures were generated with MOLSCRIPT (Kraulis, 1991).

group is only stabilized by hydrophobic interactions with the same hydrophobic cavity close to the side chains of Leu 149(143) and Leu 156(151). The water molecule (WAT 972) which formed a hydrogen bond with the carbonyl oxygen of the *tert*-butoxycarbonyl group at pH 5.0 is not observed in the complex structure at pH 7.5.

DISCUSSION

Reaction Modes. The products of inactivation are very different when PPE is inactivated by Boc-ALA2-ALA1-NHO-Nb at different pHs, even though the binding modes of the peptide part of the inactivator are similar (Figure 4). At pH 5, the product is a hydroxylamine derivative of Ser 203(195) at the active site of PPE. In contrast, at pH 7.5, the inactivator forms a carbamate derivative with the same serine residue. In both complex structures, the inactivators bind on the S′ side of the active site. For comparison, the structure of subtilisin inactivated by the same type of inactivator has been reported (Steinmetz et al., 1994). The inactivation was also done at pH 7.5, and the final product was interpreted as a carbamate derivative. The binding mode of the inactivator is also unusual, in that the peptide part of

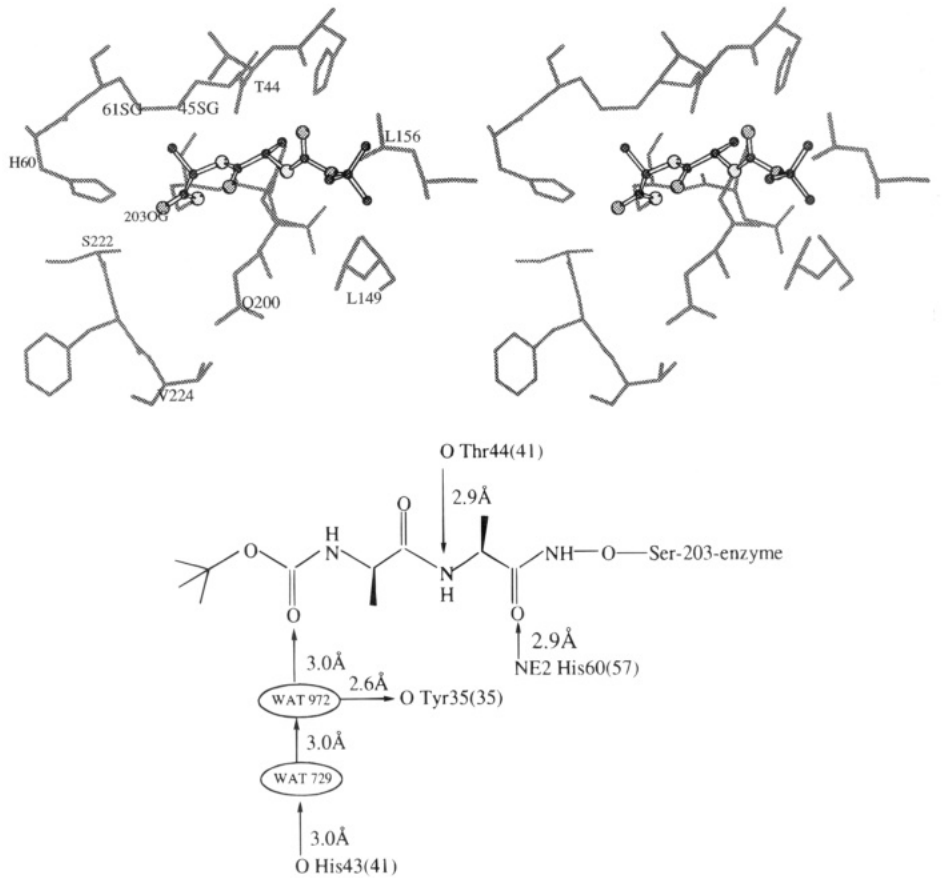

FIGURE 2: (a, top) Stereoview of the inactivator in the hydroxylamine derivative formed at pH 5, binding in the active site of PPE. The inactivator part is indicated by ball-and-sticks, the protein by solid bonds. (b, bottom) Schematic diagram of the interactions between inactivator in the hydroxylamine type complex and PPE, within hydrogen bonding distance.

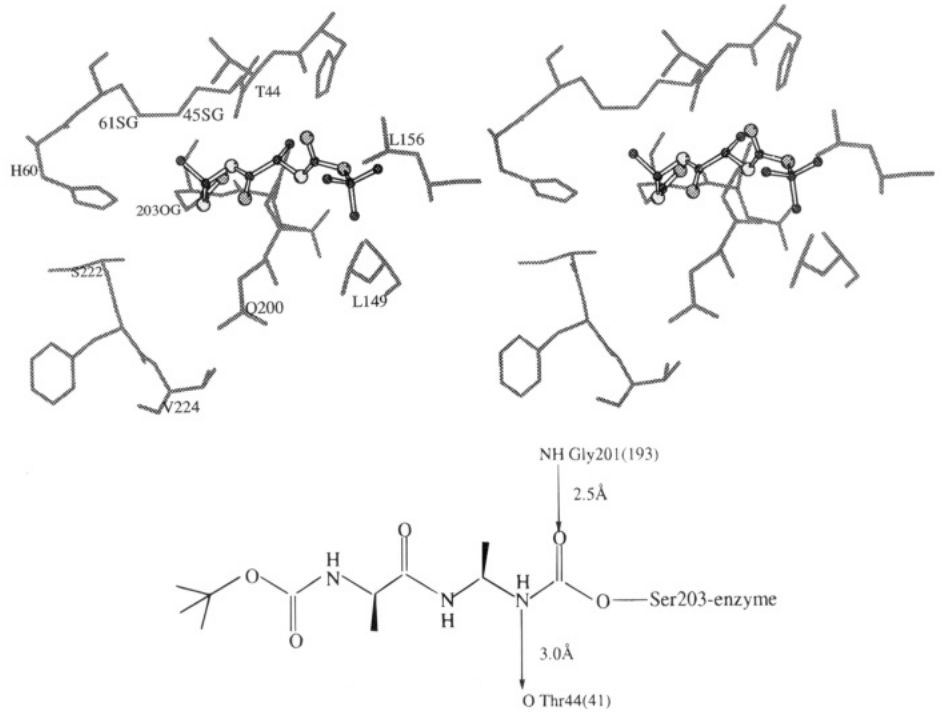

FIGURE 3: (a, top) Stereoview of the inactivator in the carbamate derivative formed at pH 7.5, binding in the active site of PPE. The inactivator part is indicated by ball-and-sticks, the protein by solid bonds. (b, bottom) Schematic diagram of the interactions between inactivator in the carbamate type complex and PPE, within hydrogen bonding distance.

the inhibitor binds in S subsites but does not form the usual antiparallel β-sheet with the protein, protruding out of the active site instead and stabilized by a network of water molecules.

These results imply that the inactivation of serine proteases by *N*-peptidyl-*O*-aroylhydroxylamine inactivators is pH dependent. PPE and subtilisin were inactivated at the same pH (7.5) with the same type of compound and gave the same

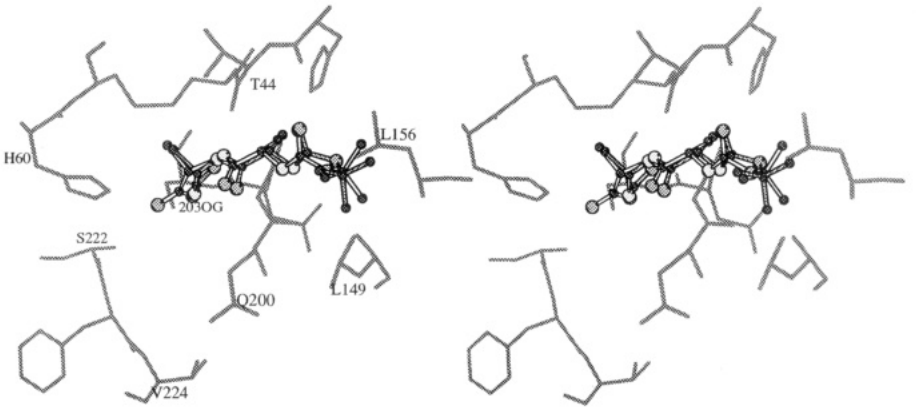

FIGURE 4: Superposition of inactivators from the hydroxylamine complex formed at pH 5 and the carbamate complex formed at pH 7.5.

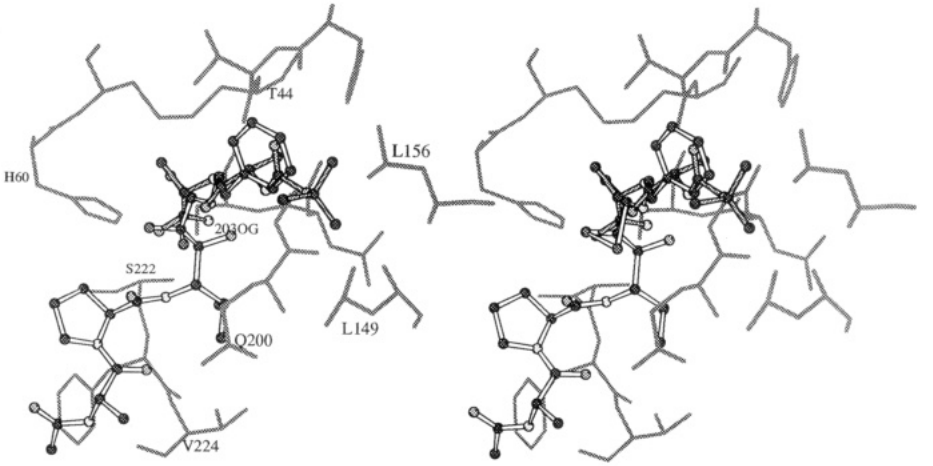

FIGURE 5: Superposition of the inactivator from the hydroxylamine complex and the inhibitor Ac-Ala-Pro-Val-difluoro-*N*-phenylethylacetamide (Takahashi et al., 1989; PDB entry no. pdb4est.ent) bound to PPE. In the structure of the Ac-Ala-Pro-Val-difluoro-*N*-phenylethylacetamide/PPE complex, the acyl-part of the inhibitor binds in S subsites in the way that is believed to represent the productive binding mode of substrates. The leaving group binds in S′ subsites. The inactivators reported here bind similarly as P′ residues of the hemiketal complex on the S′ side. The protein is represented by solid bonds, the inactivator reported here in shaded ball-and-sticks, and the hemiketal inhibitor in open ball-and-sticks.

type of product, despite the fact that the peptides have different binding modes. PPE was also inactivated at a different pH (5.0), and produced a different type of derivative, still having the same peptide binding mode as seen in the PPE−inactivator derivative at pH 7.5. This binding mode of the inactivator may be unique to elastase.

In order to answer the question of how product formation is controlled, we first have to ask whether the inactivated product comes from an enzyme-catalyzed inactivation or from inactivation by the products of nonenzymatic degradation of the inactivator. Thus, there are two possibilities. In one case, the inactivator forms the inactivating species in the active site of the enzyme, which then reacts with the enzyme in the way postulated for mechanism-based inhibitors. In the second case, the inactivator degrades in solution without help from the enzyme, and the product of degradation reacts with the enzyme.

Spontaneous degradation of a number of *N*-peptidyl-*O*-(*p*-nitrobenzoyl) hydroxamates in solution has been studied at neutral pH (Demuth et al., 1989), where the reactants exist as monoanions (pK_a ~5.5, unpublished result). In these compounds, the N^--O bond is not expected to be stable. The products of this decomposition suggest that fission of the N^--O bond generates a *p*-nitrobenzoate ion and an acyl nitrene. This nitrene intermediate is attacked rapidly by water, producing a hydroxamic acid. In the presence of an enzyme, a similar mechanism is possible. However, formation of a carbamate derivative precludes direct attack of the active site serine on the acyl nitrene. The nitrene has to rearrange first to an isocyanate followed by attack of the enzyme nucleophile. Since nitrenes are inherently unstable in aqueous solution, the reaction is expected to occur in the active site of the enzyme and inactivation can be explained by an enzyme-assisted process.

The precise mechanism which can explain the different products of inactivation at different pHs is still unclear. One possible pathway (pathway II) involves the formation of a nitrene as the first intermediate at both pH 5 and 7.5. A mechanism involving a nitrene intermediate is supported by the observation that diacylhydroxylamine reacts with water to give products that can only be explained by nitrogen−oxygen fission of the hydroxylamine moiety followed by the reaction of nitrene with water (Demuth et al., 1989). Thus, the lifetime of this nitrene intermediate determines which product will form. At pH 5, the predominant reaction is rapid formation of a covalent bond between the γ-oxygen of Ser 203(195) and the nitrene to give a hydroxylamine derivative. At pH 7.5, the predominant reaction is a Lossen-type rearrangement before attack of the serine oxygen can occur. The resulting product is a carbamate derivative derived from attack of the γ-oxygen of Ser 203(195) on the isocyanate. An alternative mechanism has been suggested

to explain the exclusive formation of a sulfenamide derivative between a peptidyl *O*-mesitoylhydroxamate and papain. In this study, the product of the reaction at pH 7 was determined by NMR. A mechanism was proposed involving migration of the enzyme thiol group from an initially formed tetrahedral adduct at the carbonyl of the P1 residue to the nitrogen of the hydroxylamine, giving the sulfenamide with loss of mesitoate as a leaving group. A similar mechanism can be proposed for the reaction of these inhibitors with serine proteases, however, only at pH 5. At more neutral pHs, this type of product is not observed with the serine proteases. Alternatively, inactivation of papain can also be explained in terms of a nitrene intermediate. The difference in product would then be due to the differences in reactivity of a thiol versus a hydroxyl group.

Binding Modes. The inactivator in both complexes is not bound as expected in the S subsites of PPE, as identified by the observed binding modes of inhibitors and substrates (Mattos et al., 1993; Ding et al., 1994) (Figure 5). Instead it is bound backward in the S′ binding sites. The interactions between polypeptides binding in the S′ subsites of serine proteases are less well-established than those in the S subsites, because the P′ residues are on the leaving group side of a substrate and the enzyme is designed to release them efficiently. Thus, they are rarely observed structurally. An example of an inhibitor that binds to both types of sites (S and S′) of PPE was reported by Takahashi (1988) in the structure of Ace-Ala-Pro-Val-difluoro-*n*-phenylethylaceamide bound to PPE. This inhibitor forms a stable complex with PPE by means of a covalent bond to Ser 203(195) Oγ, resulting in a hemiketal derivative. In this complex structure, the difluoro group binds in the S1′ site, and the phenylethyl moiety binds in the S2′ site. There are no hydrogen bonds or strong interactions between the inhibitor and PPE on the S′ sides. This structure can be used as the basis for identifying the S1′ and S2′ subsites of elastase. According to this model, in the hydroxylamine/carbamate derivatives reported here, the inactivator is bound in a conformation that places two of the inhibitor residues into these two sites (Figure 5). The ALA1 group binds at the S1′ site and both the ALA2 and Boc group bind at the S2′ site. In both structures, a hydrogen bond (2.9 Å) between the amide nitrogen of ALA1 at S1′ and the carbonyl oxygen of Thr 44(41) was observed.

One question is left unanswered by this study. Does the inactivator first bind to the active site of the enzyme like other substrates do, followed by reaction to form the covalent derivative and conformational rearrangement to give the observed product? Or does the inactivator form a Michaelis complex in the active site of the enzyme in a configuration similar to that of the final product, and does the catalytic machinery then react with the inactivator anyway? We cannot answer this question from this crystallographic study.

Conclusion. This study shows that Boc-ALA2-ALA1-NHO-Nb inactivates PPE by the formation of a hydroxylamine type complex at pH 5 and a carbamate type complex at pH 7.5. Combined with the result of inactivation of subtilisin by the same type of inactivator (Steinmetz et al., 1994), we conclude that the final product of serine protease inactivation by hydroxylamine type inhibitors is neither enzyme specific nor controlled by mode of binding of inactivator. Instead it is pH controlled.

The inactivators in both derivatives bind in the S′ subsites of PPE instead of forming the usual antiparallel β-sheet in the S subsites. The conclusions we can draw are 2-fold: either the structure we observe does not correspond to the Michaelis complex or PPE can accommodate different ligand binding modes and still react to form a covalent complex.

ACKNOWLEDGMENT

We thank David H. Harrison for help in data collection. We also thank Gregory A. Petsko for helpful discussions.

REFERENCES

Bernstein, F. C., Koetzle, T. F., Williams, G. J. B., Meyer, E. F., Jr., Brire, M. D., Rodgers, Y. R., Kenard, O., Shimanduchi, T., & Tasumi, M. (1977) *J. Mol. Biol. 112*, 535−542.

Brünger, A. T. (1988) *J. Mol. Biol. 203*, 803−816.

Brünger, A. T., Kuriyan, J., & Karplus, M. (1987) *Science 235*, 458−460.

Clore, G. M., Gronenborn, A. M., Carlson, G., & Meyer, E. (1986) *J. Mol. Biol. 190*, 259−267.

Demuth, H.-U., Baumgrass, R., Schaper, C., Fisher, G., & Barth, A. (1988) *J. Enzyme Inhib. 2*, 129−142.

Demuth, H.-U., Schoenlein, C., & Barth, A. (1989) *Biochim. Biophys. Acta 996*, 19−22.

Demuth, H.-U., Silberring, J., & Nyberg, F. (1991) *J. Enzyme Inhib. 4*, 289−298.

Ding, X. C., Rasmussen, B. F., Petsko, G. A., & Ringe, D. (1994) *Biochemistry 33*, 9285−9293.

Fischer, G., Demuth, H.-U., & Barth, A. (1983) *Pharmazie 38*, 249−250.

Hendrickson, W. A., & Konnert, J. H. (1978) *Biomolecular Structure, Conformation, Function and evolution: Diffraction and Related Studies*, pp 43−57, Pergamon Press, Oxford.

Jones, T. A. (1985) *Methods Enzymol. 115*, 157−171.

Kabsch, W. (1988) *J. Appl. Crystallogr. 21*, 67−71, 916−924.

Konnert, J. H., & Hendrickson, W. A. (1980) *Acta Crystallogr. A36*, 344−350.

Kraulis, P. J. (1991) *J. Appl. Crystallogr. 24*, 946−950.

Kraut, J. (1977) *Annu. Rev. Biochem. 46*, 331−358.

Mattos, C., Rasmussen, B. F., Ding, X. C., Petsko, G. A., & Ringe, D. (1994) *Nature, Struct. Biol. 1*, 55−58.

Meyer, E. F., Radhakrishnan, R., Cole, G. M., & Presta, L. G. (1986) *J. Mol. Biol. 1989*, 533−539.

Meyer, E. F., Cole, G. M., & Radhakrishnan, R. (1988) *Acta Crystallogr. B44*, 26−38.

Powers, J. C., Oleksyszyn, J., Narasimhan, S. L., & Kam, C.-M. (1990) *Biochemistry 29*, 3108−3118.

Robinson, V. J., Coles, P. J., Smith, R. A., & Krantz, A. (1991) *J. Am. Chem. Soc. 113*, 7760−7761.

Smith, R. A., Coles, P. J., Spencer, R. W., Copp, L. J., Jones, C. S., & Krantz, A. (1988) *Biochem. Biophys. Res. Commun. 155*, 1201−1206.

Steinmetz, A. C. U., Demuth, H.-U., & Ringe, D. (1994) *Biochemistry 33*, 10535−10544.

Takahashi, L. H., Radhakrishnan, R., Rosenfield, R. E., Jr., Meyer, E. F., Jr., & Trainor, D. A. (1988) *J. Am. Chem. Soc. 111*, 3368−3374.

Tronrud, D. E., TenEyck, L. F., & Matthews, B. W. (1987) *Acta Crystallogr. A43*, 489−501.

BI9428078